Chapter 1

Degradation of Toxic Organic Contaminants by Graphene Cathode in an Electro-Fenton System

Liu Shuan, Zhao Xia, Jiang Xin, Zhao Xiaorong,
Pu Jibin, Wang Liping and Zhou Kaihe

Additional information is available at the end of the chapter

http://dx.doi.org/10.5772/67492

Abstract

A novel composite electrode was constructed by pressing graphene and CuO, using a cathode in an electro-Fenton (EF) system. Cyclic voltammetry, charge/discharge curve and electrochemical impedance spectroscopy (EIS) were used to characterize the composite electrode. The degradation of a toxic organic contaminant, Terramycin, by EF system was studied in an undivided electrolysis cell. The possible degradation products of Terramycin were studied by a Fourier transform-infrared spectrum, and the findings showed that the structure of Terramycin was damaged. The variations of hydrogen peroxide and the relative content of hydroxyl radical (·OH) during the degradation process were traced by enzyme catalysis method and fluorescence spectrometry. The results showed that the electro-catalytic degradation of Terramycin occurred by an ·OH radical mechanism. More importantly, this as-prepared cathode was very stable and could be reused without any catalytic activity decrease, suggesting its potential application in the wastewater treatment.

Keywords: Terramycin, CuO-graphene electrode, electro-Fenton system, hydrogen peroxide, hydroxyl radicals introduction

1. Introduction

Persistent organic pollutants (POPs) resist conventional chemical and biological treatments and accumulate in the aquatic environment after discharge. They tend to be liposoluble and undergo food chain amplification and, if toxic, threaten human health [1, 2].

Electro-Fenton (EF) reaction is one of the most widely used advanced oxidation processes (AOPs) for the destruction of a wide range of recalcitrant organic contaminants such as antibiotics that cannot be eliminated biologically in wastewater [3–5]. In the EF systems, they have the ability to in situ generate highly potent chemical oxidants such as ·OH, which is strong enough to non-selectively oxidize most organic as well as some inorganic compounds [6]. H_2O_2 is simultaneously produced in an aqueous medium at the cathode by the $2e^-$ reduction of the dissolved molecular oxygen (Eq. (1)), and ·OH is formed from the Fenton's reagent according to the following reaction (Eqs. (2, 3)) [7].

$$O_2 + 2H^+ + 2e \rightarrow H_2O_2\,(\text{acidic}) \quad (1a)$$

$$O_2 + 2H_2O + 2e \rightarrow H_2O_2 + 2OH^-\,(\text{basic}) \quad (1b)$$

$$H_2O_2 + 2e \rightarrow 2{\cdot}OH \quad (2)$$

$$H_2O_2 + Fe^{2+} \rightarrow Fe^{3+} + OH^- + {\cdot}OH \quad (3)$$

Therefore, cathode materials determine the efficiency of the EF system. Usually, carbon materials with excellent characteristics of conductivity, gas diffusion, adsorption and catalysis are chosen as cathode materials. Graphene, an excellent functional material, has been widely used in super capacitors [8], transistors [9, 10], fuel cells [11], etc., but as electrode materials in electro-catalytic degradation of organic matter, very few have been reported. In this research, a new CuO-graphene electrode was constructed by pressing nano-CuO and pure graphene together. The electro-catalytic characteristics of the CuO-graphene electrode were studied using cyclic voltammetry, time power method and electrochemical impedance spectroscopy, respectively. In the EF system, the CuO-graphene electrode acted as the cathode and the pt net as the anode to degrade Terramycin. The concentration of Terramycin in the oxidative degradation was traced by HPLC. The variations of hydrogen peroxide and the relative content of hydroxyl radical during the degradation process were traced by enzyme catalysis method and fluorescence spectrometry, and the oxidation mechanism of Terramycin by EF system was studied.

2. Preparation and characterization of CuO-graphene cathode

In this section, we will describe the preparation and the properties of CuO-graphene cathode and discuss its electro-catalytic characterization. Graphene (layer of 8–10, diameter of 20–40 μm, thickness of 6–15 nm, purity 99.5%) was purchased from Ningbo Morsh Technology Company in China. Nano-CuO was prepared by the hydrothermal method. The CuO-graphene composite cathode was prepared by loading CuO onto graphene powder. CuO and graphene were mixed in an ethanol/PTFE emulsion (60% by volume), sonicated for 5 min to disperse the mixture completely, and then dried at 50°C to form a dough-like paste. Two pieces of the paste were fixed on a stainless steel mesh current collector and pressed at 30 MPa for 2 min. The electrode was refluxed in acetone for 24 h to remove ethanol and surface PTFE. The dimensions of the composite cathode were 1.0 cm^2 × 5.0 mm (see **Figure 1**; the composite cathode was firmly compressed with the edge sealed with epoxy coating to yield an exposed area of 1 cm^2).

http://dx.doi.org/10.5772/67492

Figure 1. The photograph of the CuO-graphene electrode.

CHI-660E electrochemical station was employed to study the electro-catalytic characteristics of the CuO-graphene cathode at room temperature. A Pt net (99.99% purity, Tianjin Aida Technology Co., Ltd.) of 2.0 cm^2 in area was used as the counter electrode and a saturated calomel electrode (SCE) equipped with a Luggin capillary as the reference electrode. **Figure 2** displayed the cyclic voltammetry curves of the CuO-graphene electrode under neutral pH conditions after being scanned eight times. The electrode showed good electro-catalytic properties under the working voltage. There were two pairs of redox peaks in the system medium. The current peak at 0.246 V vs. SCE is produced by the cathodic reduction of O_2 to H_2O_2 and that at −0.231 V vs. SCE is produced by the cathodic reduction of H^+ to H_2 [12]. Thus, there are two degradation pathways that may occur in the EF system. One is the anodic electrochemical oxidation process on the Pt anode [13] and the other is the cathodic ·OH oxidation process in which the CuO-graphene cathode catalyzes the two-electron reduction of O_2 to H_2O_2 under certain potential, and the H_2O_2 may be converted to ·OH [14].

$$H_2O_2 + e \rightarrow OH^- + \cdot OH \tag{4}$$

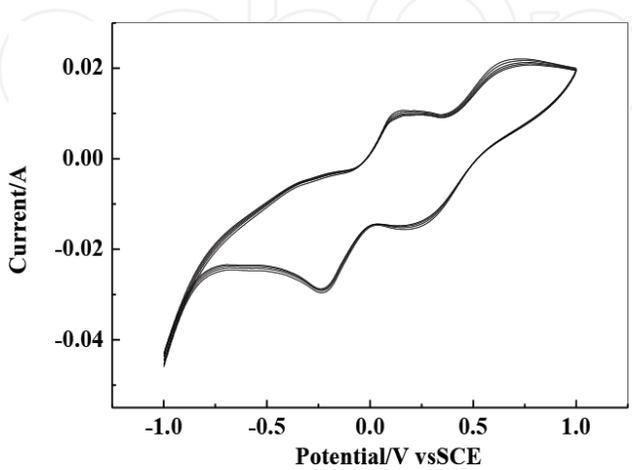

Figure 2. The CV curves of CuO-graphene cathode in a 10 g/L Na_2SO_4 solution, with a scan rate of 1 mV/s.

The specific capacitance is the ratio of capacity and mass of the electrode, which could represent the reversibility and stability of the as-prepared electrode while charging/discharging. **Figure 3** showed the charge/discharge curve of CuO-graphene cathode in a 10 g/L Na_2SO_4 solution with a scan rate of 1 mV/s, a current of 10 mA and a potential range of −0.8 to +0.8 V (vs. SCE). After nine repeated cycles, the charging and discharging curve still showed good symmetry, the potential was essentially linear with time and the charge-discharge curve slope dV/dt was still constant, suggesting that the CuO-graphene cathode material had a good reversibility [15].

EIS is a rapid, in situ and non-destructive technique for investigating the electrochemical properties of the electrode surface and affording information on the impedance changes of the electrode surface during the modification process [16, 17]. **Figure 4** illustrated the Nyquist diagrams and Bode plots of the CuO-graphene cathode under different reduction potentials in 10 g/L Na_2SO_4 solution. It can be seen that all the impedance spectra exhibited a capacitive semicircle at the medium-high frequency and a bigger capacitive semicircle at the medium-low frequency. Two-time constants were observed in the Bode plots under different reduction potential. R_s is the solution resistance and the medium-high frequency circuit Q_m–R_m corresponds to the capacitance and the ohmic process within the porous structure; the medium-low frequency circuit Q_{dl}–R_{ct} is the double-layer capacitance and the kinetic process of electrochemical reaction (the O_2 reduction into H_2O_2) [18, 19]. For the capacitive loops, the coefficients n_1 and n_2 represent a depressed feature in the Nyquist diagram. The EIS data was simulated by ZSimpWin software through **Figure 5** [20, 21]. It was seen that the equivalent circuit fitted the experimental data well in most of the frequency ranges (**Figure 4**), suggesting that the equivalent circuit (**Figure 5**) was suitable.

According to the fitted results in **Table 1**, the values of R_s remained constant as the reduction potential increased. When the reduction potential changed from 0 to −250 mV, the R_{ct} values

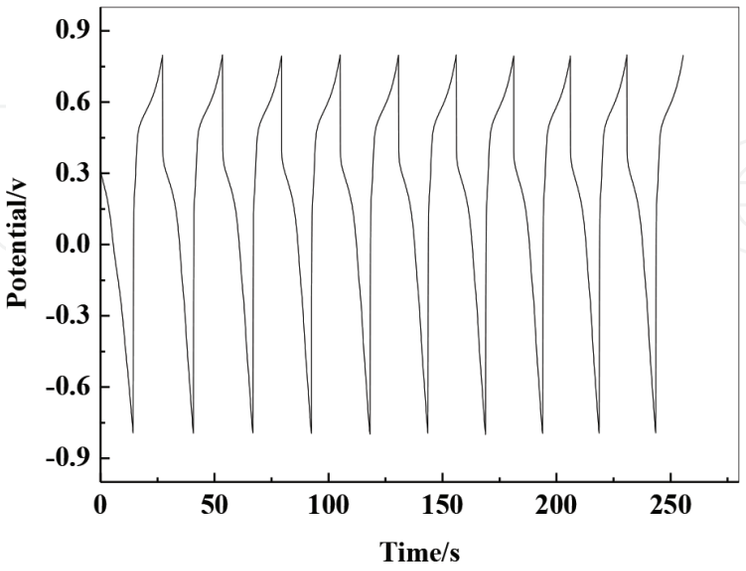

Figure 3. The charge-discharge of the CuO-graphene cathode in a 10 g/L Na_2SO_4 solution, at a scan rate of 1 mV/s and current of 10 mA.

http://dx.doi.org/10.5772/67492

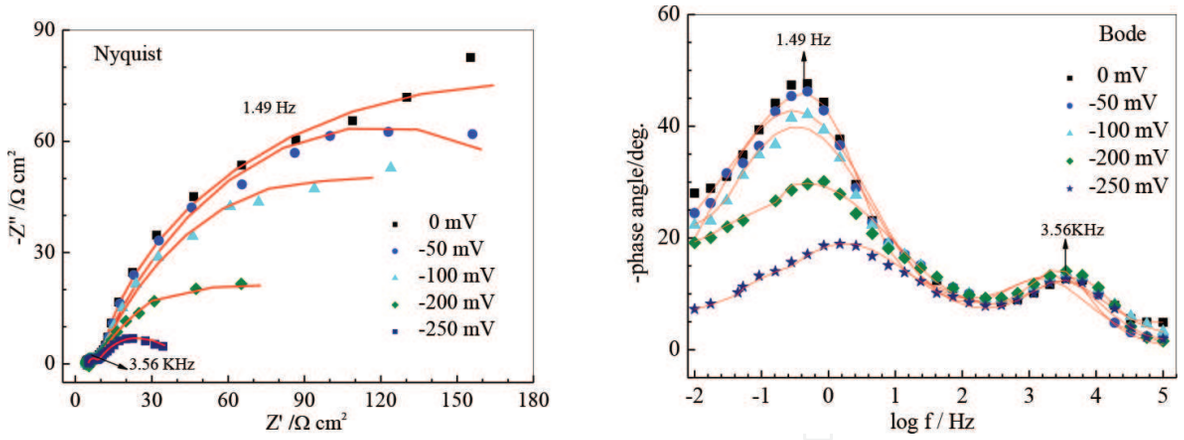

Figure 4. The experimental (dots with different symbols) and the fitted (solid lines) EIS curves of the CuO-graphene cathode according to the presented equivalent circuit immersed in a 10 g/L Na_2SO_4 solution under different reduction potentials.

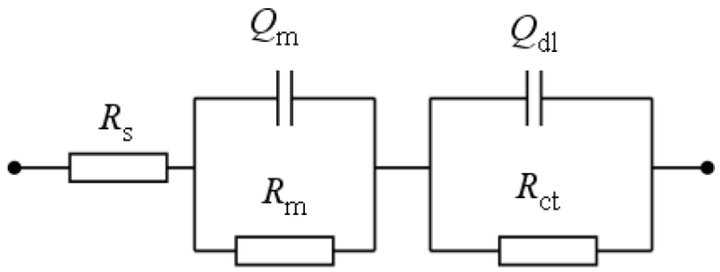

Figure 5. The equivalent circuit models used to fit the experiment impedance data of the CuO-graphene cathode in a 10 g/L Na_2SO_4 solution.

decreased from 420.5 to 30.12 Ω cm², and R_m values decreased from 9.51 to 3.45 Ω cm², indicating that the reduction rate of O_2 into H_2O_2 on CuO-graphene cathode was very rapid under higher reduction potential, that is to say, the degradation rate based on Cuo-graphene cathode of EF system increased with reduction potential. It should be noted that higher reduction potential might cause the electrolysis of water [22].

Cathodic potential	R_s Ω cm²	Q_m (F cm⁻²)	n_1	R_m (Ω cm²)	Q_2 (F cm⁻²)	n_2	R_{ct} (Ω cm²)
0 mV	3.724	0.0092	0.80	9.51	0.00071	0.89	402.5
−50 mV	4.37	0.00031	0.77	6.06	0.015	0.66	223.9
−100 mV	3.91	0.000054	0.81	4.70	0.016	0.65	175.9
−200 mV	4.40	0.000025	0.99	2.83	0.021	0.54	108.4
−250 mV	4.04	0.000064	0.86	3.45	0.019	0.59	30.12

Table 1. EIS fitting parameters of the CuO-graphene cathode under different reduction potentials (0, −50, −100, −200 and −250 mV) in 10 g/L Na_2SO_4 solution.

3. Degradation mechanism of Terramycin in EF system

3.1. The degradation process of Terramycin in EF system

The EF system degradation of Terramycin was performed in an undivided cell (50 mL) with a two-electrode system at room temperature. A Pt net (99.99% purity, Tianjin Aida Technology Co., Ltd) of 1.0 cm^2 in area was used as the anode. The as-prepared CuO-Graphene electrode was employed as the cathode. The initial concentration of Terramycin was 20 ug/L. Na_2SO_4 aqueous solution of 10 g/L was used as the electrolyte to increase the conductivity. The initial pH of the Terramycin solution was neutral at 7.0. The solution was magnetically stirred at room temperature during the whole reaction period. Before degradation experiments, the system was stirred for 40 min to establish adsorption/desorption equilibrium between the solution and electrodes, and then different voltages were applied and 1 mL samples were collected and analyzed with HPLC spectra to examine the decomposition of Terramycin.

Analysis of HPLC: The mobile phases were pump-mixed dynamically from oxalic buffers (including 1 mmol/L of EDTA solution) and acetonitrile at specified compositions. The flow rate was 1.0 mL/min and the injection volume was 20 mL. The UV detection was at 254 nm, and the column temperature was maintained at 35°C [23].

Figure 6 showed the changes of HPLC chromatograms of Terramycin in the EF system under 5 V in 10 g/L of Na_2SO_4 aqueous solution. The mobile phase was V(acetonitrile): V(oxalic buffers) = 30: 70 of mixture, adding a little EDTA in the mobile phase in order to chelate with Cu^{2+}/Cu^{+} which were corroded from the CuO-Graphene electrode. It was observed that the peak of Terramycin at the retention time of 3.06 min gradually decreased with time, and disappeared thoroughly after 180 min, which means that the tetracycline had degraded completely.

3.2. Effect of applied potential on degradation of Terramycin in EF system

Figure 7 depicted the degradation rate of Terramycin in the EF system under different applied potentials. As we know, the generation rate of H_2O_2 on the cathode depended on the applied potential, and the degradation efficiency of the EF system is proportional to the quantity of ·OH produced by Fenton's reaction [24, 25]. When no power was applied, no H_2O_2 was

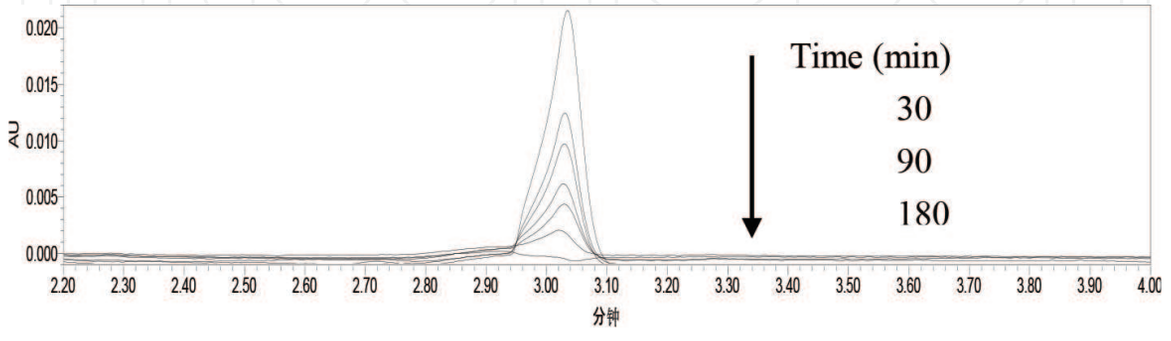

Figure 6. HPLC spectra of Terramycin during degradation in the EF system with the CuO-Graphene cathode: initial concentration of Terramycin, 20 ug/L; electrolyte, 10 g/L of Na_2SO_4; applied potential, 5 V.

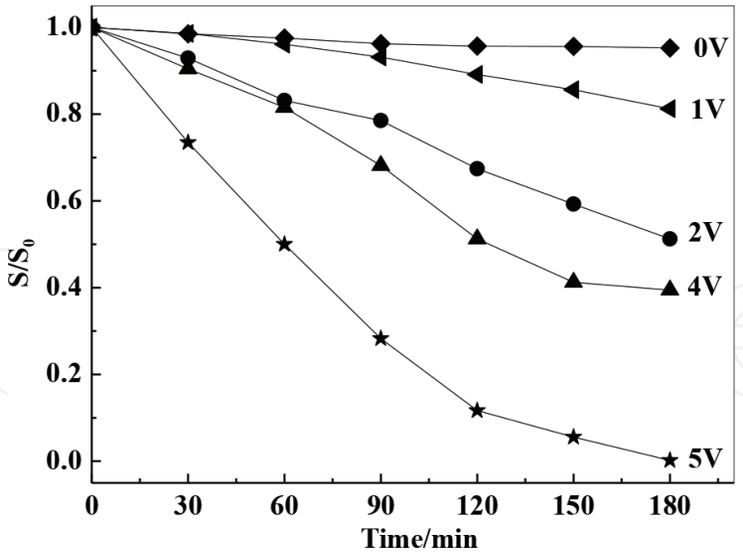

Figure 7. Effects of applied potentials on Terramycin degradation in the EF system with the CuO-Graphene cathode. S: HPLC peak area and S_0: the initial peak area. Initial tetracycline concentration, 20 ug/L; initial pH = 7.0; electrolyte, 10 g/L Na_2SO_4.

generated in EF system and there was no Terramycin degradation in the blank solution [26, 27]. The degradation efficiency of Terramycin increased with the addition of applied potentials; only 60.6% of Terramycin decomposed in 180 min at 4 V, and when the potential reached 5 V, Terramycin decomposed 100% in 180 min. This phenomenon can be ascribed to the fact that a higher potential leads to higher H_2O_2 formation rate, resulting in an increased rate of ·OH formation from Fenton's reaction. When the applied potential exceeded 5 V, the electrolysis of water increased.

3.3. Concentration of oxidizing species during degradation of Terramycin

The effectiveness of the Fenton reaction depends on the catalytic generation of H_2O_2, which yields the highly reactive species, ·OH radical, that oxidizes organic material non-selectively. In the EF system, the electrogenerated levels of H_2O_2 and ·OH determine the rate and efficiency of Terramycin degradation. **Figure 9** displayed the concentration changes of H_2O_2 and relative content of ·OH as the degradation reaction proceeded.

Analysis of H_2O_2: The concentration of H_2O_2 was determined by the oxidation of peroxidase catalytic method. The reaction was carried out in a colorimetric tube (10 mL). 30 μL of 1.0 mg/mL horseradish peroxidase (POD), 1 mL of NaH_2PO_4-NaOH buffer solution (pH = 6.80), 150 μL of 10.0 mg/mL N,N-diethyl-p-phenylenediamine (DPD) and 1 mL sample were added into the colorimetric tube in turns. After oxidation for 15 min, the concentration of H_2O_2 was analyzed spectroscopically at the wavelength of 510 nm [28]. Analysis of ·OH: The relative content of ·OH was determined by fluorescence spectrometry. 1 mL of 0.01 mol/L benzoic acid and 1 mL sample from Fenton's reaction system was added into a 10 mL colorimetric tube and the volume was kept constant at 5mL; after a reaction time of 10 min, the content of ·OH was analyzed with an excitation wavelength of 309 nm and an emission wavelength of 410 nm, and the slit width of excitation and emission was 5 nm [29].

Little amounts of H_2O_2 and ·OH were detected in the blank solution (the applied potential was 0 V). With the electrolysis performed, the amount of H_2O_2 concentration accumulated in the EF system was calculated. As 5 V was applied, the concentration of H_2O_2, generated by cathodic reduction, increased with time. After 90 min, the H_2O_2 concentration reached 2.3 × 10^{-5} mol/L and fluctuated over time. This indicates that the H_2O_2 production increased in the beginning and then was consumed in the degradation of Terramycin. These results were in good agreement with the previous experimental studies by Wang [14], who conducted diethyl phthalate degradation using a self-made Pd/C gas-diffusion cathode and a Ti/IrO_2/RuO_2 anode. By comparing **Figure 8a** and **b**, it can be seen that the electrogenerated H_2O_2 in the EF system was quickly converted to ·OH. The content of ·OH increased by prolonging the electrolysis time and then reached a steady state after about 120 min [30, 31]. The degradation of Terramycin in the EF system was in accordance with the characteristic of the Fenton reaction, indicating that the degradation process involves ·OH [32, 33].

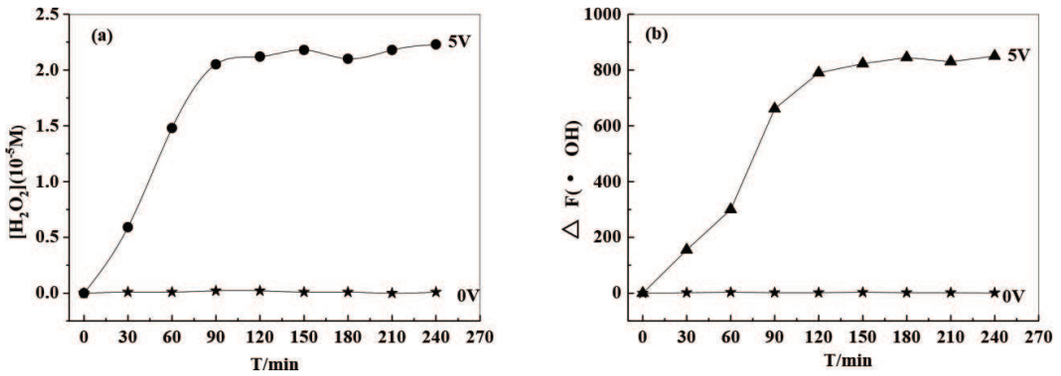

Figure 8. Evolution of the concentration of H_2O_2 (a) and relative content of ·OH (b) during the degradation of Terramycin in the EF system, initial Terramycin concentration, 20 μg/L; initial pH = 7.0; electrolyte, 10 g/L Na_2SO_4.

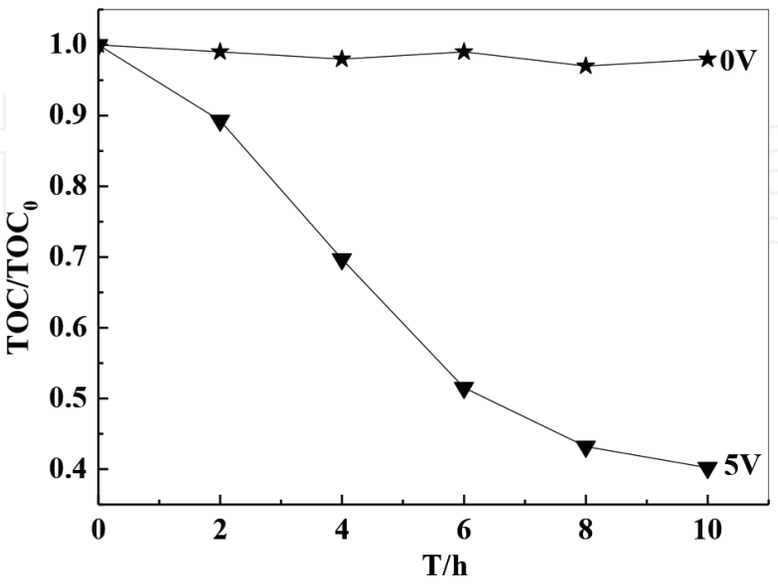

Figure 9. Evolution of TOC for the degradation of Terramycin, initial tetracycline concentration, 60 ug/L; initial pH = 7.0; electrolyte, 10 g/L Na_2SO_4.

3.4. The deep oxidation of Terramycin in EF system

In order to measure the extent of Terramycin mineralization during the degradation process, the TOC change of solution was tracked during degradation, and the results were displayed in **Figure 9**. The TOC did not change when no power was applied to the electrode, but as a voltage of 5 V was applied, the mineralization rate of Terramycin was 59.8% in 10 h. These results indicated that the EF system not only degraded the Terramycin but also oxidized over half of the Terramycin into CO_2 (mineralization) [34, 35].

3.5. IR spectra of the Terramycin in EF system during degradation

IR spectra were used to identify non-mineralized products as the degradation proceeded and the results are displayed in **Figure 10** [36–38]. Initially, the bands 1450 and 930 and 750–800 cm^{-1} corresponded to benzene ring vibration and C—H in the benzene ring plane bending vibration, respectively. The in-plane bending vibration absorption peak at 1620–1650 cm^{-1} indicated the existence of O═C—NH_2, and the bands at 1310 and 1180–1240 cm^{-1} indicated the existence of (). With the photoelectron-catalytic reaction proceeding, bands of () vibrations disappeared after 10 h, and at the same time, a new band at 1110 cm^{-1}emerged, which indicated that the tertiary amine was wiped off from the skeleton molecule of Terramycin and degraded into small amine molecules. Meanwhile, the 750–800 and 930 cm^{-1} bands of characteristic vibrations in the benzene ring bond disappeared. These results showed that the Terramycin aromatic structure was damaged.

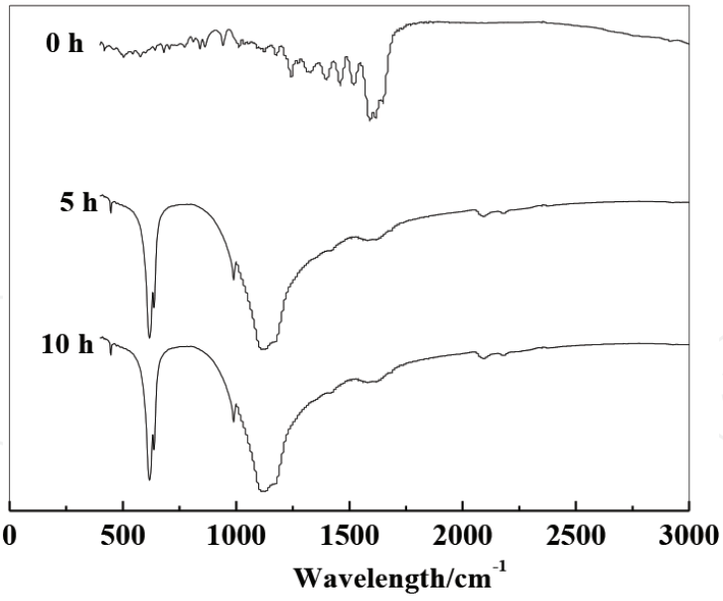

Figure 10. The IR spectra of the Terramycin in the EF system after different times.

3.6. The stability of CuO-graphene electrode in EF system

The stability of the electrode is very important for its application in environmental technology [39, 40]. In order to study the stability of CuO-graphene electrode, the degradation of Terramycin

with the same CuO-graphene electrode under the same conditions is also evaluated. **Figure 11** showed the degradation stability of the CuO-graphene cathode over five cycles in the EF system. After being reused five times, the degradation rates of Terramycin for cycle one, two, three, four and five were 97.84, 95.67, 95.21, 96.54 and 93.88%, respectively, indicating that the CuO-graphene electrode was stable and reusable.

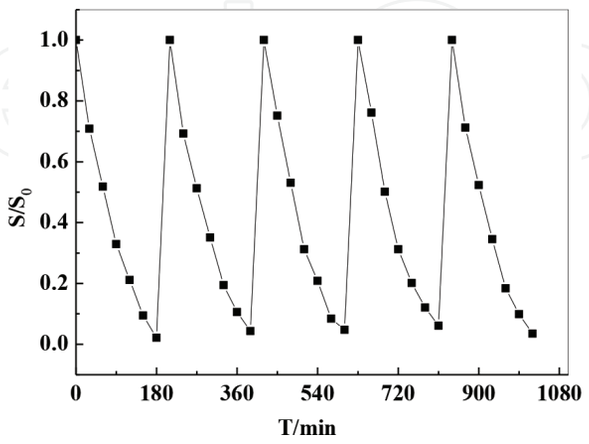

Figure 11. The degradation stability of the CuO-graphene cathode over five cycles in the EF system, initial Terramycin concentration, 20 μg/L; initial pH = 7.0; applied potential, 5 V; electrolyte, 10 g/L of Na_2SO_4.

4. Conclusion

A new cathode-CuO-graphene electrode was prepared by pressing nano-CuO and graphene. The degradation of Terramycin was investigated in an undivided electrolysis cell with a CuO-graphene cathode and Pt net anode. The electro-catalytic performance of the CuO-graphene cathode was studied by cyclic voltammetry, charge/discharge curve and electrochemical impedance spectroscopy. The primary conclusions were listed as follows:

(1) The CuO-graphene cathode was stable and exhibited high catalytic activity in neutral Na_2SO_4 solution.

(2) Under the optimal conditions of using 10 g/L of supporting electrolyte Na_2SO_4 at 5 V with a pH of 7.0 and reaction time of 180 minutes, respectively, up to 100% of 20 ug/L of Terramycin degraded.

(3) Terramycin can be mineralized to carbon dioxide and small molecules; this new EF system may soon be developed for other toxic organic contaminants degradation.

Acknowledgements

The authors wish to acknowledge the financial support of the National Science Foundation of China (No. 41506098), Zhejiang Province Preferential Postdoctoral Science Foundation

(No. BSW1502160) and Open Fund Project of the Key Laboratory of Marine Materials and Related Technologies (LMMT-KFKT-2014-008) in the Chinese Academy of Sciences.

Author details

Liu Shuan[1], Zhao Xia[1], Jiang Xin[1], Zhao Xiaorong[2]*, Pu Jibin[1]*, Wang Liping[1] and Zhou Kaihe[3]

*Address all correspondence to: rongrong315@ctgu.edu.cn; pujibin@nimte.ac.cn.

1 Key Laboratory of Marine Materials and Related Technologies, Zhejiang Key Laboratory of Marine Materials and Protective Technologies, Ningbo Institute of Materials Technologies and Engineering, Chinese Academy of Sciences, Ningbo, China

2 College of Hydraulic and Environmental Engineering, China Three Gorges University, Yichang, China

3 State Grid Zhejiang Electric Power Corporation Ningbo Power Supply Company, Ningbo, China

References

[1] AM Díez, O Iglesias, E Rosales, et al. Optimization of two-chamber photo electro Fenton reactor for the treatment of winery wastewater. Process Safety and Environmental Protection, 101 (2016) 72–79.

[2] RS Rocha, FL Silva, RB Valim, et al. Effect of Fe^{2+} on the degradation of the pesticide profenofos by electrogenerated H_2O_2. Journal of Electroanalytical Chemistry, 783 (2016) 100–105.

[3] J Meijide, J Gómez, M Pazos, et al. Degradation of thiamethoxam by the synergetic effect between anodic oxidation and Fenton reactions. Journal of Hazardous Materials, 319 (2016) 43–50.

[4] HC Lan, JF Li, M Sun, et al. Efficient conversion of dimethylarsinate into arsenic and its simultaneous adsorption removal over FeCx/N-doped carbon fiber composite in an Electro-Fenton process. Water Research, 100 (2016) 57–64.

[5] H Nakagawa, S Takagi, J Maekawa et al. Fered-Fenton process for the degradation of 1,4-dioxane with an activated carbon electrode: a kinetic model including active radicals. Chemical Engineering Journal, 296 (2016) 398–405.

[6] PY Liang, M Rivallin, S Cerneaux, et al. Coupling cathodic Electro-Fenton reaction to membrane filtration for AO7 dye degradation: a successful feasibility study. Journal of Membrane Science, 510 (2016) 182–190.

[7] JH Shen, YF Li, YH Zhu, et al. Aerosol synthesis of Graphene-Fe_3O_4 hollow hybrid microspheres for heterogeneous Fenton and Electro-Fenton reaction. Journal of Environmental Chemical Engineering, 4 (2016) 2469–2476.

[8] NL Chen, YP Ren, PP Kong, et al. In situ one-pot preparation of reduced graphene oxide/polyaniline composite for high-performance electrochemical capacitors. Applied Surface Science, 392 (2017) 71–79.

[9] JP Cheng, L Liu, KY Ma, et al. Hybrid nanomaterial of α-$Co(OH)_2$ nanosheets and few-layer graphene as an enhanced electrode material for supercapacitors. Journal of Colloid and Interface Science, 486 (2017) 344–350.

[10] K Deshmukh, MB Ahamed, KK Sadasivuni, et al. Graphene oxide reinforced poly (4-styrenesulfonic acid)/polyvinyl alcohol blend composites with enhanced dielectric properties for portable and flexible electronics. Materials Chemistry and Physics, 186 (2017) 188–201.

[11] K Kim, J Bae, MY Lim, et al. Enhanced physical stability and chemical durability of sulfonated poly(arylene ether sulfone) composite membranes having antioxidant grafted graphene oxide for polymer electrolyte membrane fuel cell applications. Journal of Membrane Science, 525 (2017) 125–134.

[12] XR Zhao, S Liu, YP Huang. Removing organic contaminants by an Electro-Fenton system constructed with graphene cathode. Toxicological & Environmental Chemistry, 98 (2015) 530–539.

[13] P Canizares, JA Domingues, MA Rodrigo, et al. Effect of the current intensity in the electrochemical oxidation of aqueous phenol wastes at an activated carbon and steel anode. Industrial and Engineering Chemistry Research, 38 (1999) 3779–3785.

[14] H Wang, DZ Sun, ZY Bian. Degradation mechanism of diethyl phthalate with electro-generated hydroxyl radical on a Pd/C gas-diffusion electrode. Journal of Hazardous Materials, 180 (2010) 710–715.

[15] S Liu, XR Zhao, HY Sun, et al. The degradation of tetracycline in a photoelectro-Fenton system. Chemical Engineering Journal, 231 (2013) 441–448.

[16] L Gu, S Liu, HC Zhao, et al. Facile preparation of water-dispersible graphene sheets stabilized by carboxylated oligoanilines and their anticorrosion coatings. ACS Applied Materials and Interfaces, 7 (2015) 17641–17648.

[17] S Liu, L Gu, HC Zhao, et al. Corrosion resistance of graphene-reinforced waterborne epoxy coatings. Journal of Materials Science & Technology, 32 (2016) 425–431.

[18] S Liu, HY Sun, HJ Fan et al. Effects of pH and Cl^- concentration on corrosion behavior of the galvanized steel in simulated rust layer solution. Corrosion Science, 65 (2012) 520–527.

[19] H Wei, D Ding, S Wei, et al. Anticorrosive conductive polyurethane multiwalled carbon nanotube nanocomposites. Journal of Materials Chemistry A, 1 (2013) 10805–10813.

[20] HY Sun, S Liu, LJ Sun. A comparative study on the corrosion of galvanized steel under simulated rust layer solution with and without 3.5 wt% NaCl. International Journal of Electrochemical Science, 8 (2013) 3494–3509.

[21] MM Wind, HJW Lenderink. A capacitance study of pseudo-fickian diffusion in glassy polymer coatings. Progress in Organic Coatings, 28 (1996) 239–250.

[22] Y Fan, ZH Ai, LZ Zhang. Design of an Electro-Fenton system with a novel sandwich film cathode for wastewater treatment. Journal of Hazard Materials, 176 (2010) 678–684.

[23] RP Li, Y Zhang, YP Huang, et al. Development and validation of a hydrophilic interaction liquid chromatographic method for determination of aromatic amines in environmental water. Journal of Chromatography A, 1217 (2010) 1799–1805.

[24] M Zarei, A Niaei, D Salari, et al. Removal of four dyes from aqueous medium by the peroxi-coagulation method using carbon nanotube-PTFE cathode and neural network modeling. Journal of Electroanalytical Chemistry, 639 (2010) 167–174.

[25] D Salari, A Niaei, A Khataee, et al. Electrochemical treatment of dye solution containing C.I. Basic Yellow 2 by the peroxi-coagulation method and modeling of experimental results by artificial neural networks. Journal of Electroanalytical Chemistry, 629 (2009) 117–125.

[26] L Fu, S J You, GQ Zhang, et al. Degradation of azo dyes using insitu Fenton reaction incorporated into H_2O_2-producing microbial fuel cell. Chemical Engineering Journal, 160 (2010) 164–169.

[27] GQ Zhang, FL Yang, MM Gao, et al. Electro-Fenton degradation of azo dye using polypyrrole/anthraquinonedisulphonate composite film modified graphite cathode in acidic aqueous solutions. Electrochimica Acta, 53 (2008) 5155–5161.

[28] H Bader, V Sturzenegger, J Hoigne. Photometric method for the determination of low concentrations of hydrogen peroxide by the peroxidase catalyzed oxidation of *N*,*N*-p-phenylene-diamine. Water Research, 22 (1988) 1109–1115.

[29] S Liu, Y Gu, SL Wang, et al. Degradation of organic pollutants by a Co_3O_4-graphite composite electrode in an Electro-Fenton-like system. Chinese Science Bulletin, 58 (2013) 2340–2346.

[30] HY Zhao, Y Chen, QS Peng, et al. Catalytic activity of MOF(2Fe/Co)/carbon aerogel for improving H_2O_2 and ·OH generation in solar photo–electro–Fenton process. Applied Catalysis B: Environmental, 203 (2017) 127–137.

[31] N Flores, I Sirés, JA Garrido, et al. Degradation of trans-ferulic acid in acidic aqueous medium by anodic oxidation, Electro-Fenton and photoelectro-Fenton. Journal of Hazardous Materials, 319 (2016) 3–12.

[32] ZH Ai, LR Lu, JP Li, et al. Fe@Fe_2O_3 core–shellnanowires as iron reagent. 1. Efficient degradation of Rhodamine B by a novel sono-Fenton process. Journal of Physical Chemistry C, 111 (2007) 4087–4093.

[33] ZH Ai, LR Lu, JP Li, et al. Fe@Fe_2O_3 core–shell nanowires as iron reagent. 2. An efficient and reusable sono-Fenton system working at neutral pH. Journal of Physical Chemistry C, 111 (2007) 7430–7436.

[34] RS Rocha, FL Silva, RB Valim, et al. Effect of Fe^{2+} on the degradation of the pesticide profenofos by electrogenerated H_2O_2. Journal of Electroanalytical Chemistry, 783 (2016) 100–105.

[35] PY Liang, M Rivallin, S Cerneaux, et al. Coupling cathodic Electro-Fenton reaction to membrane filtration for AO7 dye degradation: a successful feasibility study. Journal of Membrane Science, 510 (2016) 182–190.

[36] F Sopaj, N Oturan, J Pinson, et al. Effect of the anode materials on the efficiency of the Electro-Fenton process for the mineralization of the antibiotic sulfamethazine. Applied Catalysis B: Environmental, 199 (2016) 331–341.

[37] C Espinoza, J Romero, L Villegas, et al. Mineralization of the textile dye acid yellow 42 by solar photoelectro-Fenton in a lab-pilot plant. Journal of Hazardous Materials, 319 (2016) 24–33.

[38] Y Zhang, MM Gao, XH Wang, et al. Enhancement of oxygen diffusion process on a rotating disk electrode for the Electro-Fenton degradation of tetracycline. Electrochimica Acta, 182 (2015) 73–80.

[39] OG Rodríguez, JA Bañuelos, AE Ghenymy, et al. Use of a carbon felt-iron oxide air-diffusion cathode for the mineralization of Malachite Green dye by heterogeneous Electro-Fenton and UVA photoelectro-Fenton processes. Journal of Electroanalytical Chemistry, 767 (2016) 40–48.

[40] W Chen, XL Yang, JF Huang, et al. Iron oxide containing graphene/carbon nanotube based carbon aerogel as an efficient E-Fenton cathode for the degradation of methyl blue. Electrochimica Acta, 200 (2016) 75–83.